J. Fluid Mech. (1980), *vol.* 96, *part* 2, *pp.* 375–393
Printed in Great Britain

Onset of convection in a layered porous medium heated from below

By R. McKIBBIN AND M. J. O'SULLIVAN
Department of Theoretical and Applied Mechanics,
University of Auckland, New Zealand

(Received 19 January 1979 and in revised form 9 May 1979)

The formalism required to determine the criterion for the onset of convection in a multi-layered porous medium heated from below is developed using a straightforward linear stability analysis. Detailed results for two- and three-layer configurations are presented. These results show that large permeability differences between the layers are required to force the system into an onset mode different from a homogeneous system.

1. Introduction

The problem of the onset of convection in a fluid-saturated porous layer heated from below is of considerable interest because of its connection with the mathematical modelling of geothermal fields and also because it is one of the simplest problems involving hydrodynamic instability. The earliest work on the problem by Horton & Rogers (1945) and Lapwood (1948) established that convection occurs in a horizontal porous layer, confined between isothermal impermeable boundaries, for Rayleigh numbers above the critical value of $4\pi^2$. Subsequent research has been directed at both the problem of the finite amplitude motion for Rayleigh numbers above $4\pi^2$ and also more complicated onset problems. The present work is in the latter category.

Lapwood considered a horizontal, homogeneous, isotropic layer with isothermal boundaries, an impermeable bottom boundary and either an impermeable or constant pressure top. This work was generalized by Gheorghitza (1961) for two particular inhomogeneous problems. The first problem involved two homogeneous layers with a slightly different permeability in the top layer from that in the bottom. In the second problem a layer with a very weak linear inhomogeneity in permeability was considered.

Wooding (1959) considered the analogous problem of convection induced by a solute concentration gradient for a vertical cylindrical tube. He also modified the analysis of Lapwood (Wooding 1960) for the case where an upflow of fluid gives rise to a steady-state temperature profile of an exponential form.

Prat (1966) investigated the effect of a uniform transverse flow on the onset problem for a homogeneous layer, finding that the critical Rayleigh number was unchanged but a modified flow pattern resulted. The more complicated problem of thermohaline convection was considered by Nield (1968) who as part of his work considered more general thermal and fluid boundary conditions for the thermal convection problem.

Westbrook (1969) used energy methods to confirm the stability results of the small-disturbance linear analysis used by Lapwood and the other workers mentioned above.

0022-1120/80/4373-8210 $02.00

The method developed by Westbrook allowed for a general equilibrium state whereas earlier work, except for that of Prat and Wooding, assumed that before the onset of convection the fluid was at rest with the temperature determined from conduction theory (usually linear). A simple problem of this more general type, where the equilibrium state consists of a uniform upward flow through the layer, was analysed by Sutton (1970) using the linear small-perturbation approach. Beck (1972) used the same energy method approach as Westbrook to examine the effect of confining lateral boundaries on the onset of convection, obtaining the critical Rayleigh number as a function of the geometry of the porous box considered.

In all the above work, a simple linear relationship between fluid density and temperature was assumed. Sun, Tien & Yen (1972) derived a modified onset condition for the case of a fluid, such as water at low temperatures, which has a density maximum. Recently Straus & Schubert (1977) have introduced further physical realism into the onset problem by considering the exact dependence on temperature and pressure of fluid viscosity and density. Schubert & Straus (1977) also considered the onset of two-phase convection.

Consideration of the effect of anisotropy of the porous medium on the criterion for the onset of convection has recently been made by several authors. Castinel & Combarnous (1975) considered the effect of anisotropic permeability while Epherre (1975) added anisotropy in thermal diffusivity. Tyvand (1977) considered the effects of cross-flow, anisotropic permeability and velocity dependent diffusion (dispersion) coefficients.

Numerous works on finite amplitude convection have also considered various complications of the basic homogeneous fluid layer case [see for example Elder (1967), Straus (1974), Caltagirone (1975), Joseph (1976) and Schubert & Straus (1978)]. Experimental verification of Lapwood's (1948) result by Schneider (1963), and Katto & Masuoka (1967) has been carried out and several later experimental investigations of finite amplitude convection have also confirmed the result. Yen (1974) experimentally verified the analysis of Sun *et al.* for the onset of convection of fluid with a density maximum.

In all the work mentioned above the porous layer was assumed to be homogeneous or, in the case of Gheorghitza, weakly inhomogeneous. Three works on finite amplitude convection have considered inhomogeneous layers. Donaldson (1962) carried out a numerical investigation of convection in a two-layer system for the special case of an impermeable but thermally conducting bottom layer. Ribando & Torrance (1976) considered an exponential variation in the ratio of viscosity to permeability. Very recently finite amplitude convection for a three-layer system was numerically investigated by Rana (1977). However no study of the onset of convection in a general inhomogeneous porous layer has been reported. Since in a geothermal context inhomogeneity, particularly layering, is common, the problem is of practical importance. The present work develops the formalism required to determine the criterion for the onset of convection in an inhomogeneous multi-layered porous medium. The analysis presented is quite general and can readily be applied to any number of layers. In the present work detailed results for two- and three-layer configurations are presented. These represent model geothermal fields where a permeable zone is overlaid by a less permeable layer or where a permeable aquifer occurs in the interior of a matrix with a different permeability.

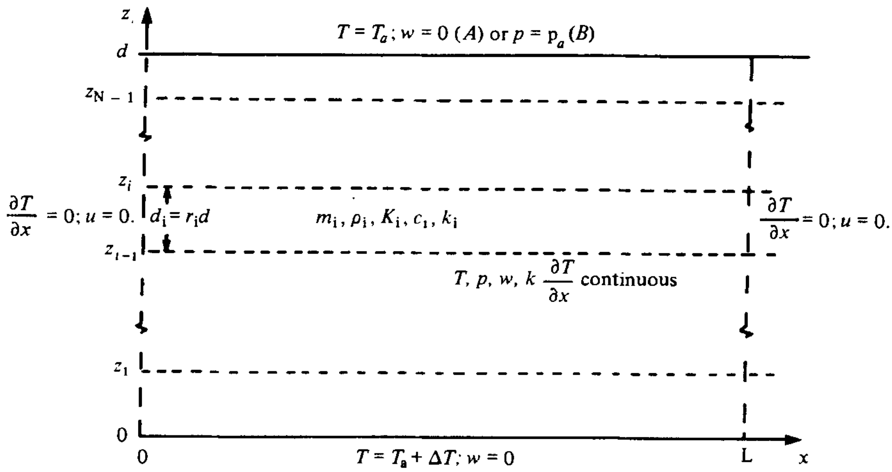

FIGURE 1. Schematic diagram of configuration considered – a porous medium comprising N homogeneous horizontal layers.

2. Problem formulation

A saturated permeable layer of total thickness d, consisting of N separate homogeneous layers is considered. The thickness, permeability and thermal conductivity may vary from layer to layer. The system is bounded below (beneath layer 1) by an impermeable isothermal surface at a temperature $T_a + \Delta T$. Here T_a is the temperature of the top surface (atmospheric) which is considered to be either impermeable (case A) or at a constant pressure (case B) (see figure 1).

Within a typical stratum, layer i, of thickness d_i, the usual equations of conservation of mass and energy and Darcy's law are assumed to hold:

$$m_i \partial\rho/\partial t + \nabla . \mathbf{v} = 0, \tag{1}$$

$$\partial/\partial t[m_i \rho c T + (1-m_i)\rho_i c_i T] + \nabla . (cT\mathbf{v}) = k_i \nabla^2 T, \tag{2}$$

$$\nabla p = \rho \mathbf{g} - \nu/K_i \mathbf{v}. \tag{3}$$

Here m_i, K_i, ρ_i, c_i are respectively the porosity, permeability, density and specific heat of the unsaturated porous medium in layer i, k_i is the thermal conductivity of the saturated medium, ρ, c, ν, $\mathbf{v}$ are respectively the density, specific heat, kinematic viscosity and mass flux vector of the fluid and T and p are the temperature and pressure at a point within the saturated porous medium. The acceleration due to gravity is represented by the vector $\mathbf{g}$.

The density is assumed to vary linearly with temperature,

$$\rho = \rho_a[1 - \alpha(T - T_a)],$$

where α is a constant and ρ_a is the density of the fluid at temperature T_a.

In studying the onset of convection in this system using linear stability methods, only steady solutions of (1)–(3) are of interest. Also in a linear stability analysis it is sufficient to consider two-dimensional motion. Whether the preferred motion is in fact two-dimensional rolls or has some three-dimensional form can only be determined by analysis of the finite amplitude behaviour of the system (see Straus 1974 for example).

Therefore in the following analysis the two-dimensional region $0 < x < L$, $0 < z < d$ is considered. On the lateral boundaries, corresponding either to the limits of each convection cell or possibly to some real physical confinement, conditions of no fluid flow and no heat flow are imposed. Taking $\mathbf{v} = (u, 0, w)$ and assuming all variables depend only on x and z, (1)–(3), for layer i, become:

$$\frac{\partial u}{\partial x}+\frac{\partial w}{\partial z} = 0, \tag{4}$$

$$c\left(u\frac{\partial T}{\partial x}+w\frac{\partial T}{\partial z}\right) = k_i\left(\frac{\partial^2 T}{\partial x^2}+\frac{\partial^2 T}{\partial z^2}\right), \tag{5}$$

$$\frac{\partial p}{\partial x} = -\frac{\nu}{K_i}u, \tag{6}$$

$$\frac{\partial p}{\partial z} = -\rho_a[1-\alpha(T-T_a)]g-\frac{\nu}{K_i}w, \tag{7}$$

for $0 < x < L$, $z_{i-1} < z < z_i$, where $z_i = \sum_{j=1}^{i} d_j$. Note that for steady flows the use of mass flows as variables avoids the need to use the Boussinesq approximation.

The thermal and fluid boundary conditions on the bottom and top of the system are, respectively:

$$T = T_a+\Delta T \quad \text{and} \quad w = 0 \quad \text{on} \quad z = 0,$$

$$T = T_a \quad \text{and} \quad \begin{cases} w = 0 & \text{on} \quad z = d \quad \text{case } A, \\ p = p_a & \text{on} \quad z = d \quad \text{case } B. \end{cases}$$

At each interface continuity in temperature, pressure, vertical mass flux and vertical heat flux is assumed (Gheorghitza used the incorrect condition of continuity in horizontal velocity instead of continuity in pressure). Thus T, p, w and $cTw+k\,\partial T/\partial z$ must be continuous at each interface. Using the continuity of T and w the last condition can be simplified to requiring continuity in $k\,\partial T/\partial z$ at each interface.

The basic solution procedure to determine the condition for the onset of convection in this layered system is to investigate small perturbations to the conduction solution ($u = w = 0$). The conduction solution for the temperature T_c is a piecewise linear function given by

$$T_c = T_a+\Delta T\left(\sum_{j=i}^{N}\delta_j+\frac{z_{i-1}-z}{k_i}\right)\Big/\delta$$

for $z_{i-1} < z < z_i$ where $\delta_i = d_i/k_i$ and $\delta = \sum_{j=1}^{N}\delta_j$. This distribution corresponds to a temperature drop ΔT_i across layer i given by

$$\Delta T_i = \delta_i \Delta T/\delta.$$

Now, following the standard linear stability analysis procedure, the system is linearised by substituting $u = u'$, $w = w'$, $T = T_c+T'$ and $p = p_c+p'$ [p_c is obtained easily from T_c by using (7)] and neglecting products of the small quantities u', w', T'

and p'. It is convenient to non-dimensionalize the variables differently in each layer. For layer i the variables are defined by:

$$T_i = T'/\Delta T_i, \quad p_i = p'K_i c/\nu r_i k_i,$$

$$(u_i, w_i) = (u', w')cd/r_i k_i, \quad X = x/d,$$

and
$$Z_i = (z - z_{i-1})/d_i.$$

Here $r_i = d_i/d$, the ratio of the thickness of layer i to the total thickness. Substitution into (4)–(7), of these non-dimensionalized perturbations to the conduction solution, gives for layer i:

$$\frac{\partial u_i}{\partial X} + \frac{1}{r_i}\frac{\partial w_i}{\partial Z_i} = 0, \tag{8}$$

$$-w_i = \frac{\partial^2 T_i}{\partial X^2} + \frac{1}{r_i^2}\frac{\partial^2 T_i}{\partial Z_i^2}, \tag{9}$$

$$\frac{\partial p_i}{\partial X} = -u_i, \tag{10}$$

$$\frac{1}{r_i}\frac{\partial p}{\partial Z_i} = \frac{R_i}{r_i^2}T_i - w_i, \tag{11}$$

for $0 < X < L/d$, $0 < Z_i < 1$ and $i = 1, 2, \ldots, N$. Here the Rayleigh number for layer i, given by

$$R_i = \frac{\rho_a g K_i c\alpha \Delta T_i d_i}{\nu k_i},$$

is based on the layer depth d_i and the layer temperature drop ΔT_i.

To aid the solution of (8)–(11), an auxiliary function ϕ_i is introduced such that

$$\psi_i = -\frac{\partial \phi_i}{\partial X},$$

where ψ_i is a stream function for layer i. Then using (8) and (10) it follows that

$$p_i = \frac{1}{r_i}\frac{\partial \phi_i}{\partial Z_i}, \quad u_i = -\frac{1}{r_i}\frac{\partial^2 \phi_i}{\partial X\, \partial Z_i} \quad \text{and} \quad w_i = \frac{\partial^2 \phi_i}{\partial X^2}$$

and (8)–(11) can be simplified to give a pair of equations for ϕ_i and T_i:

$$r_i^2\frac{\partial^2 \phi_i}{\partial X^2} + \frac{\partial^2 \phi_i}{\partial Z_i^2} = R_i T_i \tag{12}$$

and
$$r_i^2\frac{\partial^2 T_i}{\partial X^2} + \frac{\partial^2 T_i}{\partial Z_i^2} = -r_i^2\frac{\partial^2 \phi_i}{\partial X^2}, \tag{13}$$

for $0 < X < L/d$, $0 < Z_i < 1$ and $i = 1, 2, \ldots, N$. The boundary conditions can be expressed in terms of the non-dimensional quantities ϕ_i, T_i as follows. On $Z_1 = 0$,

$$T_1 = 0, \quad \frac{\partial^2 \phi_1}{\partial X^2} = 0.$$

On $Z_i = 1$ or $Z_{i+1} = 0$,

$$\frac{r_i}{k_i} T_i = \frac{r_{i+1}}{k_{i+1}} T_{i+1}, \quad r_i k_i \frac{\partial^2 \phi_i}{\partial X^2} = r_{i+1} k_{i+1} \frac{\partial^2 \phi_{i+1}}{\partial X^2},$$

$$\frac{\partial T_i}{\partial Z_i} = \frac{\partial T_{i+1}}{\partial Z_{i+1}}, \quad \frac{k_i}{K_i} \frac{\partial \phi_i}{\partial Z_i} = \frac{k_{i+1}}{K_{i+1}} \frac{\partial \phi_{i+1}}{\partial Z_{i+1}},$$

for $i = 1, 2, \ldots, N-1$, and on $Z_N = 1$,

$$T_N = 0, \quad \begin{cases} \dfrac{\partial^2 \phi_N}{\partial X^2} = 0 & \text{case } A, \\[2ex] \dfrac{\partial \phi_N}{\partial Z_N} = 0 & \text{case } B. \end{cases}$$

On the lateral boundaries $X = 0$ and $X = L/d$,

$$\frac{\partial T_i}{\partial X} = 0, \quad \frac{\partial \phi_i}{\partial X} = 0.$$

3. Solution procedure

The boundary conditions on $X = 0, L/d$ lead to Fourier cosine series for both T_i, ϕ_i:

$$(T_i, \phi_i) = \sum_{n=1}^{\infty} (T_i^n, \phi_i^n) \cos \frac{n\pi d}{L} X,$$

where T_i^n, ϕ_i^n, $n = 1, 2, \ldots$ are functions of Z_i only (the leading terms in the series T_i^0, ϕ_i^0 both turn out to be zero and are neglected from the start). Substitution of these expansions into (12) and (13) gives

$$[D_i^2 - (n\alpha_i)^2]\,\phi_i^n = R_i T_i^n, \tag{14}$$

$$[D_i^2 - (n\alpha_i)^2]\,T_i^n = (n\alpha_i)^2 \phi_i^n, \tag{15}$$

where $D_i = d/dZ_i$, and $\alpha_i = \pi d_i/L$, for $i = 1, 2, \ldots, N$ and $n = 1, 2, \ldots$. Similar matching after substitution in the boundary conditions gives, for $n = 1, 2, \ldots$, on $Z_1 = 0$:

$$T_1^n = 0, \quad \phi_1^n = 0.$$

On $Z_i = 1$ or $Z_{i+1} = 0$,

$$\frac{r_i}{k_i} T_i^n = \frac{r_{i+1}}{k_{i+1}} T_{i+1}^n, \quad r_i k_i \phi_i^n = r_{i+1} k_{i+1} \phi_{i+1}^n,$$

$$D_i T_i^n = D_{i+1} T_{i+1}^n, \quad \frac{k_i}{K_i} D_i \phi_i^n = \frac{k_{i+1}}{K_{i+1}} D_{i+1} \phi_{i+1}^n,$$

for $i = 1, 2, \ldots, N-1$. On $Z_N = 1$,

$$T_N^n = 0, \quad \text{and} \quad \begin{cases} \phi_N^n = 0 & \text{case } A, \\ D_N \phi_N^n = 0 & \text{case } B. \end{cases}$$

Elimination of either T_i^n or ϕ_i^n from (14) and (15) gives

$$\{[D_i^2 - (n\alpha_i)^2]^2 - (n\alpha_i)^2 R_i\}\,(T_i^n, \phi_i^n) = 0. \tag{16}$$

Thus, using (14) and (15), the solutions for T_i^n and ϕ_i^n can be written in the form

$$T_i^n = A_i \sinh \beta_i Z_i + B_i \cosh \beta_i Z_i + E_i \sinh \gamma_i Z_i + F_i \cosh \gamma_i Z_i, \tag{17}$$

$$\phi_i^n = \eta_i (A_i \sinh \beta_i Z_i + B_i \cosh \beta_i Z_i - E_i \sinh \gamma_i Z_i - F_i \cosh \gamma_i Z_i)/n, \tag{18}$$

where $\beta_i = \alpha_i[n(n+\eta_i)]^{\frac{1}{2}}$ and $\gamma_i = \alpha_i[n(n-\eta_i)]^{\frac{1}{2}}$ with $\eta_i = (R_i)^{\frac{1}{2}}/\alpha_i$. Note that γ_i may be imaginary or zero with corresponding trigonometric or linear forms in (17) and (18). In (17) and (18), the wavenumber superscript 'n' has been omitted from the coefficients A_i, B_i, E_i, F_i to avoid unnecessarily cumbersome notation.

Substituting (17) and (18) into the boundary conditions gives $4N$ homogeneous linear equations in the $4N$ unknown coefficients A_i, B_i, E_i and $F_i, i = 1, 2, \ldots, N$. These are

$$B_1 + F_1 = 0, \tag{19a}$$

$$B_1 - F_1 = 0, \tag{19b}$$

$$(r_i/k_i)(A_i \sinh \beta_i + B_i \cosh \beta_i + E_i \sinh \gamma_i + F_i \cosh \gamma_i) = (r_{i+1}/k_{i+1})(B_{i+1} + F_{i+1}), \tag{19c}$$

$$r_i k_i \eta_i (A_i \sinh \beta_i + B_i \cosh \beta_i - E_i \sinh \gamma_i - F_i \cosh \gamma_i) = r_{i+1} k_{i+1} \eta_{i+1} (B_{i+1} - F_{i+1}), \tag{19d}$$

$$A_i \beta_i \cosh \beta_i + B_i \beta_i \sinh \beta_i + E_i \gamma_i \cosh \gamma_i + F_i \gamma_i \sinh \gamma_i = A_{i+1} \beta_{i+1} + E_{i+1} \gamma_{i+1}, \tag{19e}$$

$$(k_i/K_i)\eta_i(A_i \beta_i \cosh \beta_i + B_i \beta_i \sinh \beta_i - E_i \gamma_i \cosh \gamma_i - F_i \gamma_i \sinh \gamma_i) = (k_{i+1}/K_{i+1})\eta_{i+1}(A_{i+1}\beta_{i+1} - E_{i+1}\gamma_{i+1}), \tag{19f}$$

for $i = 1, 2, \ldots, N-1$, and

$$A_N \sinh \beta_N + B_N \cosh \beta_N + E_N \sinh \gamma_N + F_N \cosh \gamma_N = 0 \tag{19g}$$

and either (case A)

$$A_N \sinh \beta_N + B_N \cosh \beta_N - E_N \sinh \gamma_N - F_N \cosh \gamma_N = 0 \tag{19h}$$

or (case B)

$$A_N \beta_N \cosh \beta_N + B_N \beta_N \sinh \beta_N - E_N \gamma_N \cosh \gamma_N - F_N \gamma_N \sinh \gamma_N = 0. \tag{19i}$$

These equations can be written in matrix form as

$$\mathbf{MA} = 0, \tag{20}$$

where $\mathbf{A}^T = (A_1, B_1, E_1, F_1, A_2, B_2, E_2, F_2, \ldots, A_N, B_N, E_N, F_N)$ and the $4N \times 4N$ matrix $\mathbf{M}$ can be obtained from the (19a–i). The condition for a non-trivial solution then is $\det \mathbf{M} = 0$ which is solved here for the variable R defined by

$$R = \frac{\delta d}{\delta_1 d_1} \frac{R_1}{4\pi^2} = \frac{\rho_a g K_1 c \alpha d \Delta T}{4\pi^2 \nu k_1}.$$

This parameter R is a Rayleigh number, given in terms of the thickness and temperature drop for the whole layer and the conductivity and permeability for layer 1, divided by $4\pi^2$, which is the minimum critical value for a homogeneous layer with an impermeable top. The relationship between R_1 and R is obvious from the definition above. The Rayleigh number for each layer R_i can also be related to R_1 and then to R using the relationship

$$\frac{R_i}{R_1} = \frac{K_i d_i^2 k_1^2}{k_i^2 K_1 d_1^2}.$$

By adding and subtracting (19c) and (19d) in the right combination, formulae for B_{i+1} and F_{i+1} in terms of A_i, B_i, E_i and F_i can be obtained. Similarly, formulae for A_{i+1} and E_{i+1} follow from (19e) and (19f). These equations can then be written in the form

$$\mathbf{A}_{i+1} = \mathbf{M}_i \mathbf{A}_i, \quad i = 1, 2, \ldots, N-1, \tag{21}$$

where $\mathbf{A}_i^T = (A_i, B_i, E_i, F_i)$ and $\mathbf{M}_i$ is a 4×4 matrix whose elements are derived from (19c–f) in the straightforward manner outlined above. The two sets of boundary conditions (19a, b) and (19g–i) can be written in the form

$$\mathbf{L}_1 \mathbf{A}_1 = 0 \tag{22a}$$

and

$$\mathbf{L}_N \mathbf{A}_N = 0. \tag{22b}$$

The boundary condition (22a) gives $B_1 = F_1 = 0$ which can be combined with (21), for $i = 1$, to give

$$\mathbf{A}_2 = \mathbf{Q}_1 \begin{bmatrix} A_1 \\ E_1 \end{bmatrix} \tag{23}$$

where $\mathbf{Q}_1$ is a 4×2 matrix which can easily be derived in detail using (19c–f) for $i = 1$. Equations (21), (22b) and (23) then give the equation

$$\mathbf{L}_N \mathbf{M}_{N-1} \mathbf{M}_{N-2} \ldots \mathbf{M}_2 \mathbf{Q}_1 \begin{bmatrix} A_1 \\ E_1 \end{bmatrix} = 0,$$

which for a non-trivial solution requires the condition

$$\det(\mathbf{L}_N \mathbf{M}_{N-1} \mathbf{M}_{N-2} \ldots \mathbf{M}_2 \mathbf{Q}_1) = 0. \tag{24}$$

Since the final matrix involved is 2×2 rather than $4N \times 4N$ as in (20), it is more suitable for numerical calculations.

In all but a few very simple cases, solution requires numerical methods. This is a straightforward matter and is not discussed in detail here. An algebraic check of the methods is provided by case (A) for a homogeneous layer with equal width and depth for which $R_1 = 4\pi^2$, leading to the solution $R = 1$.

4. Numerical results

There are clearly such a wide variety of possible configurations and values of various parameters that only a small number of results can be presented. Consequently detailed analysis is confined to the two- and three-layer cases, and in particular to the case of an aquifer either overlaid ('capped') by a less permeable layer, or lying centrally between two layers of another permeable material. Since the emphasis is chosen to be on the different permeabilities of the layers, the conductivities of all the layer materials are assumed to be equal in what follows. (Results for layers of different conductivities may easily be found in the same way as those to be presented.)

The physical configuration considered for most of the calculations is a square cross-section ($L/d = 1{\cdot}0$). This choice allows a comparison of values of R as well as flow and

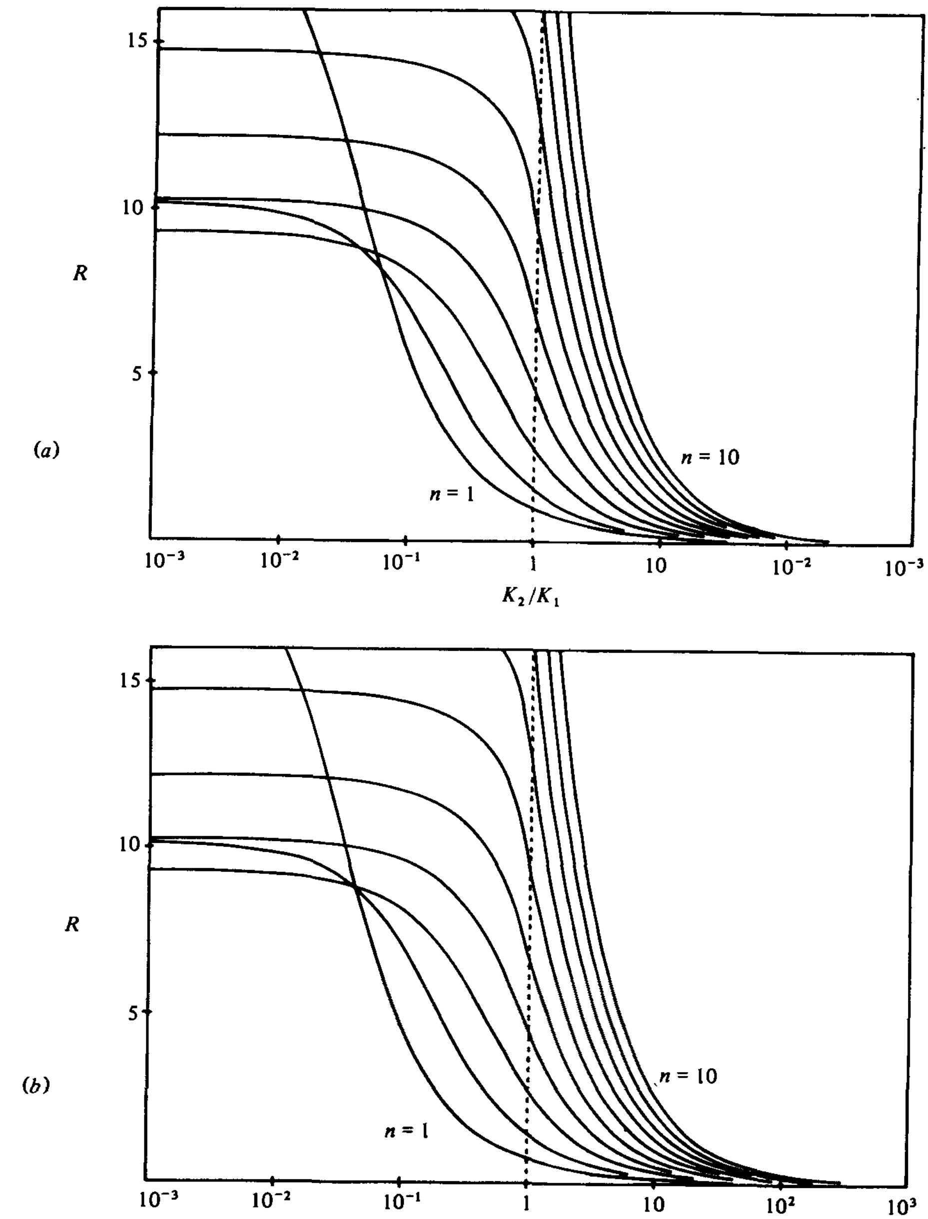

FIGURE 2. The critical Rayleigh number R for the lowest 10 horizontal wavenumbers n for a two-layer system with $L/d = 1{\cdot}0$ and $r_1 = 0{\cdot}3$. Impermeable (a) and constant pressure (b) upper boundary conditions were used.

isotherm patterns at onset for various layer combinations. Calculation of the value of R, which is a scaled Rayleigh number based on the parameters of the bottom layer, gives a comparison with the critical Rayleigh number for a homogeneous layer which is composed completely of the material of the bottom layer for the stratified case.

For a square cross-section, the number of cells in the horizontal direction which

Bottom layer thickness r_1	0·1	0·2	0·3	0·4	0·5	0·6	0·7	0·8	0·9
Horizontal wavenumber n	8	4	3	2	2	2	1	1	1
Critical Rayleigh number R	83·8	20·9	9·32	5·24	3·42	2·57	1·82	1·39	1·14

TABLE 1. Critical Rayleigh numbers for a two-layer system with square cross-section, as $K_2/K_1 \to 0$.

(a)

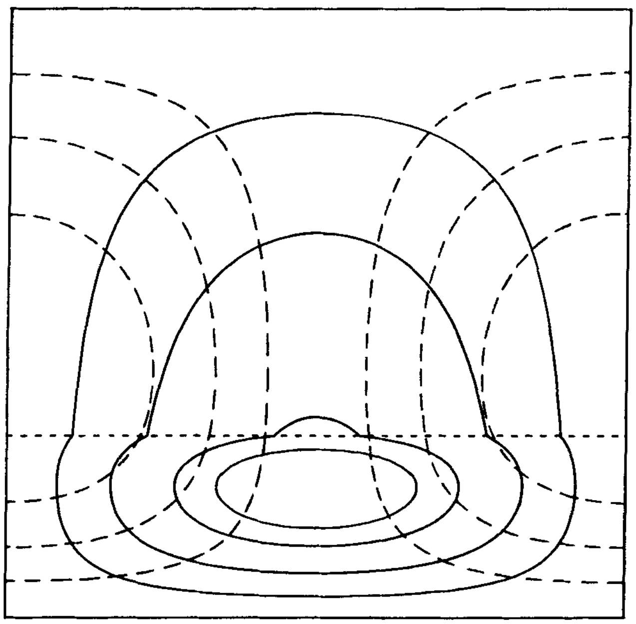

FIGURE 3(a). For legend see next page.

occur at onset varies with the layer configuration. Results are presented for this aspect of the problem for two-layer and three-layer systems with various choices of permeabilities. Also the ratio L/d is varied for a number of layer configurations to obtain the corresponding minimum Rayleigh number and therefore the critical Rayleigh number for onset in a layered system infinite in the horizontal direction.

5. The two-layer system

For a porous medium consisting of two layers, results were calculated for a variety of parameters, both for the 'closed' or impermeable top (case A) and for the 'open' or constant pressure top (case B). As mentioned above it was assumed that conductivities are equal, i.e. $k_1 = k_2$.

(b)

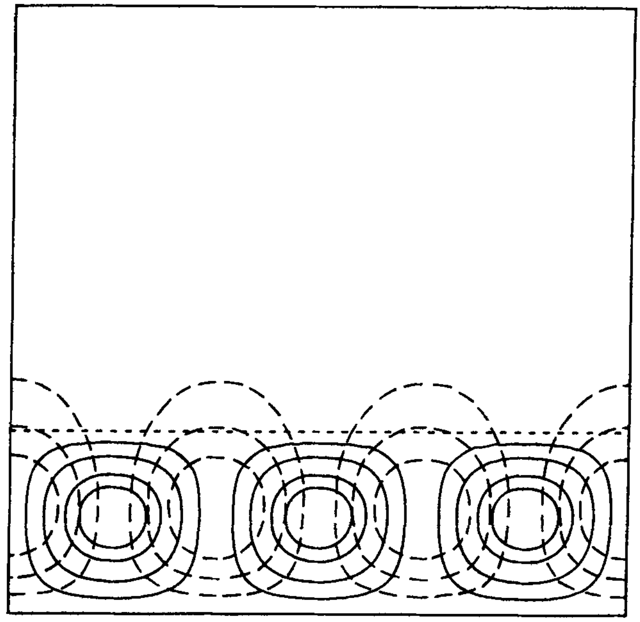

FIGURE 3. Streamlines (——) and isotherms (- - -) at onset for a two-layer system with $L/d = 1{\cdot}0$ and $r_1 = 0{\cdot}3$ and an impermeable upper boundary. (a) $K_2/K_1 = 0{\cdot}1$; (b) $K_2/K_1 = 0{\cdot}01$.

Aspect ratio $L/d = 1{\cdot}0$

For most of the results obtained, the aspect ratio was fixed at $1{\cdot}0$ corresponding to a square cross-section. For a range of different depths of the layers, values of R^n, the value of R corresponding to n cells arranged horizontally (n is the horizontal wave-number) were worked out for a wide range of the ratio of the permeabilities of the layers, K_2/K_1 ($K_2/K_1 < 1$ corresponds to a 'capped' aquifer, while $K_2/K_1 > 1$ corresponds to an aquifer overlying a less permeable, but conducting stratum).

The values of R^n for the typical configuration $L/d = 1{\cdot}0$, $r_1 = 0{\cdot}3$, $k_2/k_1 = 1{\cdot}0$, for $10^{-3} \leqslant K_2/K_1 \leqslant 10^3$ and for the lowest 10 horizontal wavenumbers n, are graphed in figure 2(a) for the 'closed top' case, and in figure 2(b) for the 'open top' case. For an impermeable top layer ($K_2/K_1 \rightarrow 0$), the preferred cell width corresponds to approximately square cells in the bottom layer. Similarly for an impermeable bottom layer ($K_2/K_1 \rightarrow \infty$), the preferred cell width corresponds to approximately square cells in the top layer. The $r_1 = 0{\cdot}3$ case gives three cells for $K_2/K_1 \rightarrow 0$ and one cell for $K_2/K_1 \rightarrow \infty$. It is noticeable that a very small permeability in the top layer is required in order to force convection to occur mainly in the bottom layer. For the closed surface case, for small values of K_2/K_1 (less than approximately $0{\cdot}040$), onset takes place for $n = 3$, while for $0{\cdot}040 < K_2/K_1 < 0{\cdot}059$ the fluid will first move in a double-celled flow, and for $K_2/K_1 > 0{\cdot}059$, the preferred flow at onset is in a single cell. Results for the 'open surface' case are similar: all values of R calculated are smaller than those for the corresponding 'closed surface' results, with the difference decreasing as $K_2/K_1 \rightarrow 0$. As K_2/K_1 becomes small, the difference between the two upper surface conditions becomes less and less important, as the whole upper layer approaches impermeability relative to the lower layer.

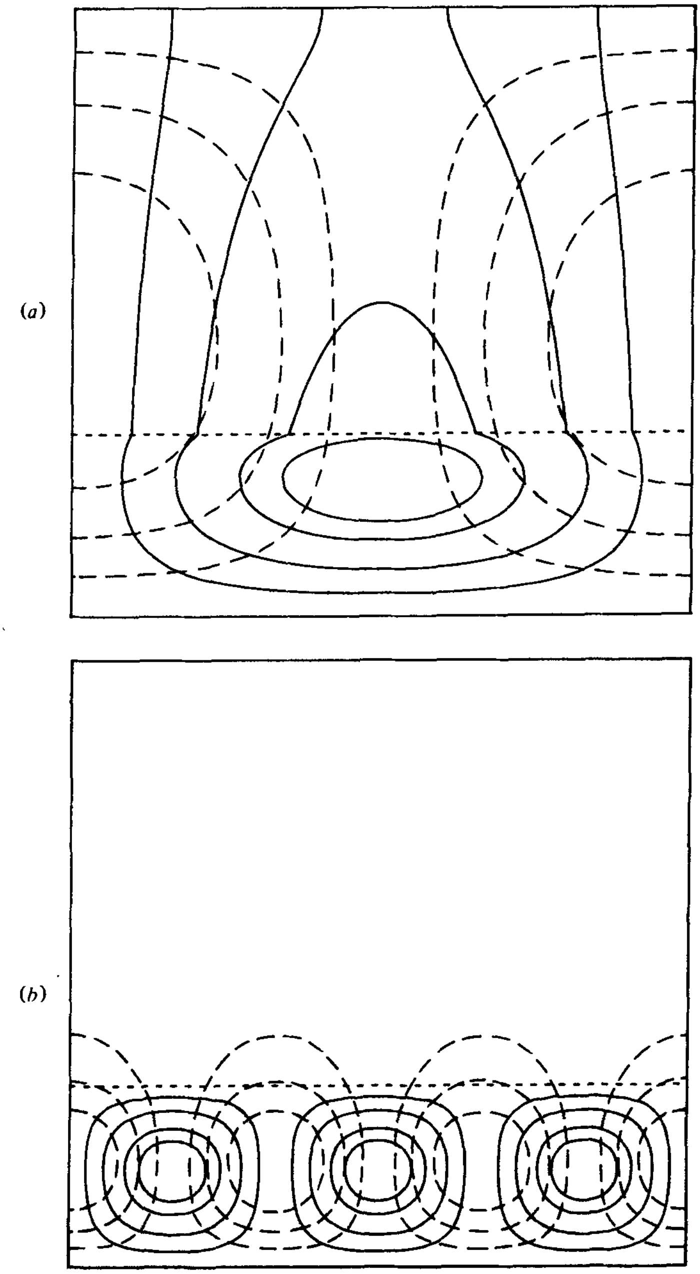

FIGURE 4. Streamlines (——) and isotherms (– – –) at onset for a two-layer system with $L/d = 1\cdot0$ and $r_1 = 0\cdot3$ and a constant pressure upper boundary. (a) $K_2/K_1 = 0\cdot1$; (b) $K_2/K_1 = 0\cdot01$.

As expected, the values of R^n decrease with increasing permeability of the upper layer (see figure 2, for example). When $K_2/K_1 = 1$ (corresponding to a homogeneous layer), the minimum value of R for the closed surface case is $R^1 = 1\cdot0$, which is the result predicted first by Lapwood (1948) and confirmed many times since.

Results for other depth ratios show a similar behaviour. For $r_1 = 0\cdot1$, for example,

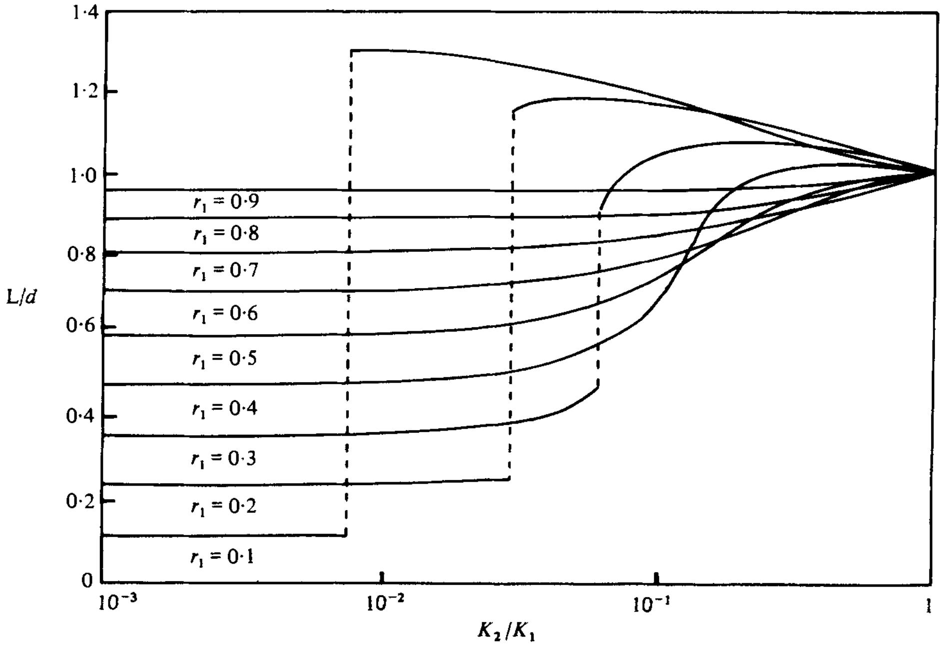

FIGURE 5. Preferred cell width at onset for an infinite two-layer system.

the wavenumber for the minimum critical value of R^n changes from $n = 1$ to $n = 8$ at $K_2/K_1 \simeq 0·008$. For a permeability ratio above this value, the flow at onset results in a single cell, while for permeability ratios below 0·008, flow begins in eight identical cells. In the limit as $K_2/K_1 \to 0$, the number of cells preferred at onset decreases with increasing r_1. Table 1 gives some values of n, together with the corresponding values of R^n (note that these values are the same for both the 'open' and 'closed surface' cases).

The values of R indicate that the presence of an upper, less permeable layer greatly increases the temperature difference required to destabilize the fluid in a two-layer system (5·655, 9·194 and 9·304 times respectively for the 'closed surface' case $r_1 = 0·3$ and $K_2/K_1 = 0·1$, 0·01 and 0·001).

Most of the flow, as may be expected, takes place within the more permeable layer. Streamlines and isotherm patterns at onset are shown in figure 3 and figure 4 for the 'closed' and 'open surface' cases for $r_1 = 0·3$, and $K_2/K_1 = 0·1$ and 0·01, the preferred number of cells being 1 and 3 respectively. It can be seen that very little flow takes place in the less permeable layer, and the cells of flow in the more permeable layer tend to form in a shape that is approximately square.

Variation in aspect ratio

Variation of preferred cell width with permeability ratio for an infinite layer is shown in figure 5. These values are found by minimizing R with respect to the aspect ratio L/d of the two-layer system.

It is interesting to note that the preferred mode at onset has the form of an approximately square cell, either occupying both layers or the bottom layer only if the top layer has a low enough permeability. As figure 5 shows there is a sudden transition

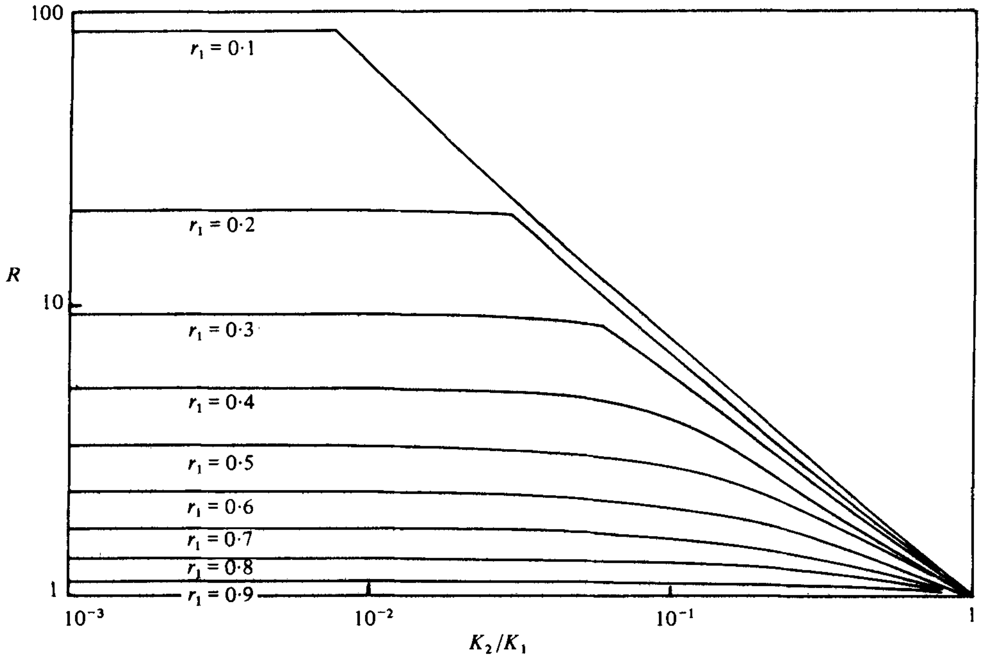

FIGURE 6. Minimum Rayleigh number at onset for an infinite two-layer system.

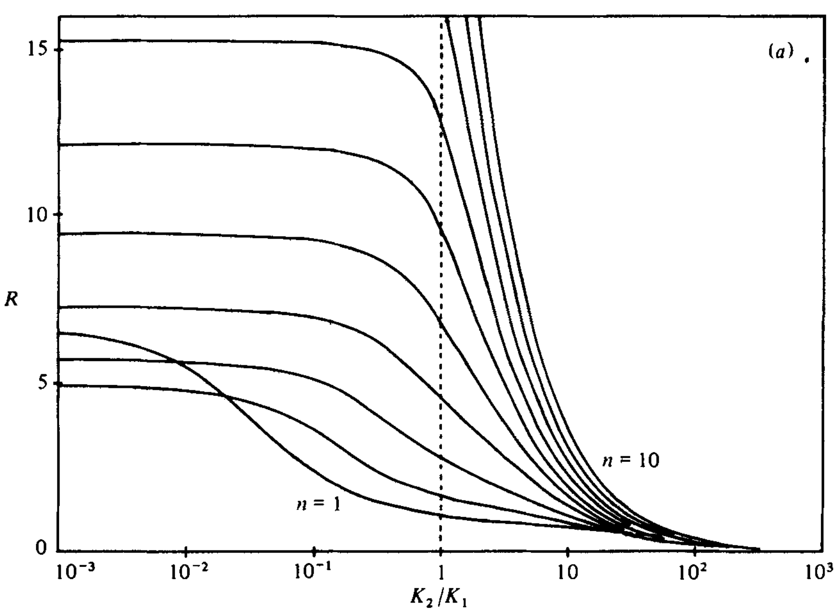

FIGURE 7 (*a*). For legend see next page.

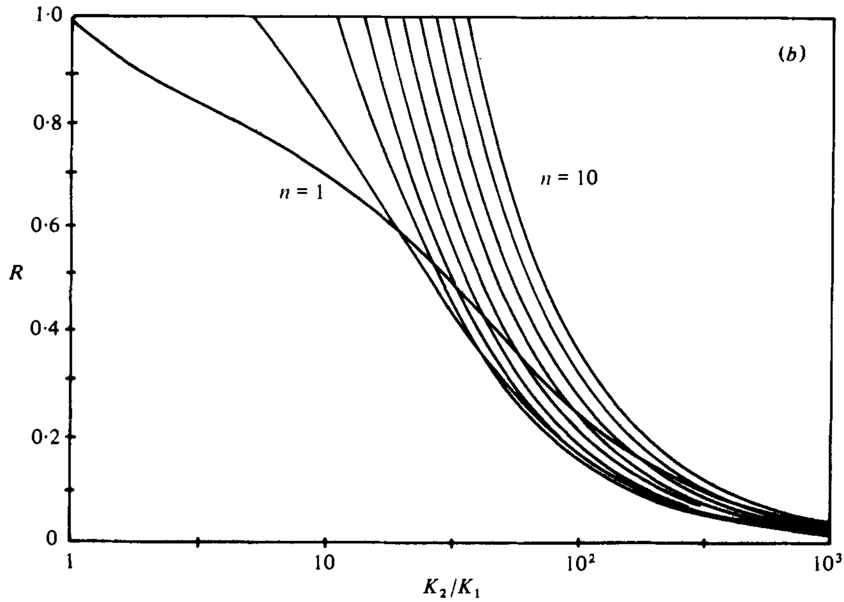

FIGURE 7. The critical Rayleigh number R for the lowest 10 horizontal wavenumbers n for a three-layer system with $L/d = 1{\cdot}0$ and $r_2 = 0{\cdot}2$ and an impermeable upper boundary.

between these two alternatives. An examination of the dependence of the critical Rayleigh number on the aspect ratio L/d shows that there are two local minima for $r_1 < 0{\cdot}4$. One of these corresponds to $L/d \simeq 1$ (square cell in the whole system) and the other to $L/d \simeq r_1$ (square cell in the bottom layer). The bifurcation shown in figure 5 results from the change-over from the first of these local minima to the second of the minima being the absolute minimum. In figure 6 the Rayleigh number for onset is shown. Again the bifurcation is clear.

6. The three-layer system

Results are presented for an aquifer of depth $r_2 = 0{\cdot}2$ sandwiched between two layers of equal depth ($r_1 = r_3 = 0{\cdot}4$), and of equal permeability, $K_3 = K_1$ (but different to that of the middle layer, K_2) and with the upper surface 'closed'. Results are presented for the square cross-section $L/d = 1{\cdot}0$ only.

The values of R^n, $n = 1, 2, \ldots, 10$ for varying permeability ratio K_2/K_1 ($= K_2/K_3$) are graphed in figure 7 ($K_2/K_1 > 1$ corresponds to a permeable aquifer lying between two less permeable, but conducting layers, while $K_2/K_1 < 1$ corresponds to a less permeable stratum cutting through a permeable matrix). The results show that a considerable permeability difference is required to change the flow from that for a homogeneous layer. For $0{\cdot}021 < K_2/K_1 < 19{\cdot}0$ onset occurs for $n = 1$. For a very impermeable ($K_2/K_1 < 0{\cdot}021$) middle layer, most of the flow occurs in the top and bottom layers with approximately square cells ($n = 2$). For a very permeable middle layer, the flow occurs mainly in the middle layer with $n = 2$ for $19{\cdot}0 < K_2/K_1 < 48{\cdot}4$ and with $n = 3$ for $48{\cdot}4 < K_2/K_1$. Similar behaviour is exhibited for cases where the middle layer is of different thickness.

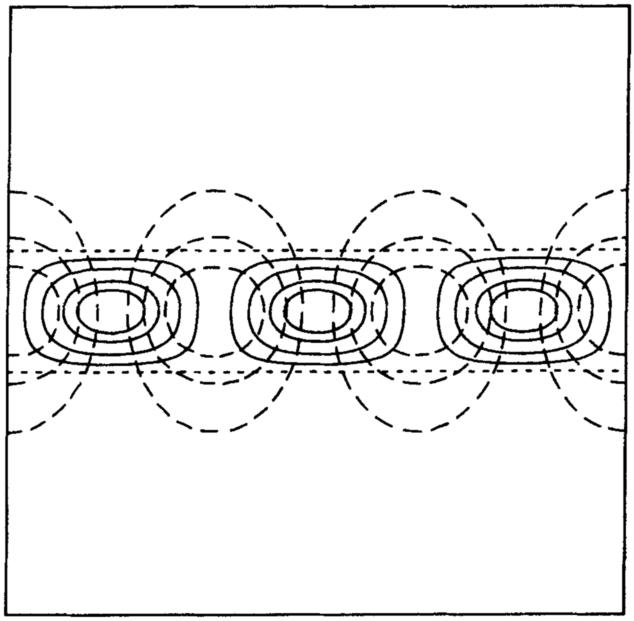

(a)

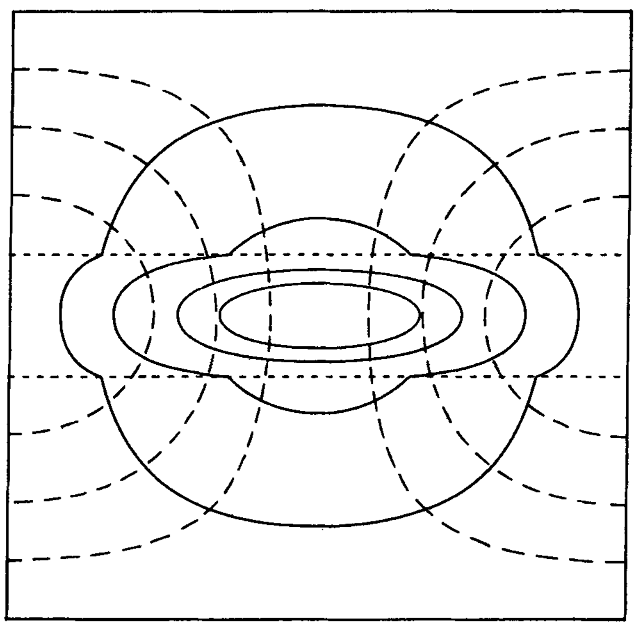

(b)

FIGURE 8 (a, b). For legend see next page.

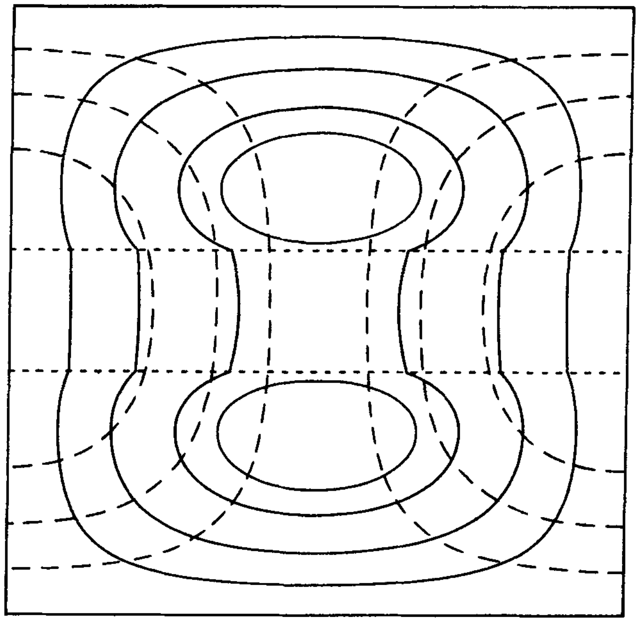

(c)

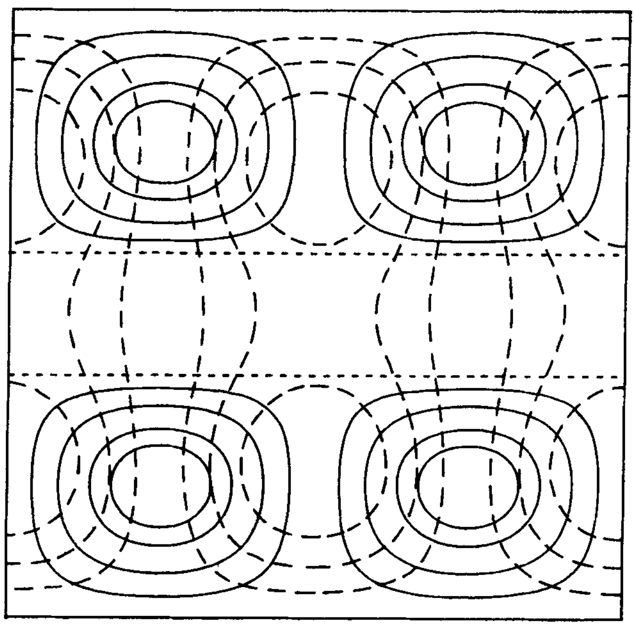

(d)

FIGURE 8. Streamlines (——) and isotherms (- - -) at onset for a three-layer system with $L/d = 1\cdot 0$ and $r_2 = 0\cdot 2$ and an impermeable upper boundary. (a) $K_2/K_1 = 100$; (b) $K_2/K_1 = 10$; (c) $K_2/K_1 = 0\cdot 1$; (d) $K_2/K_1 = 0\cdot 01$.

Again, the values of R increase with decreasing permeability of the middle layer. This result has special significance with regard to the estimation of the Rayleigh number of a natural hydrothermal system which is usually calculated from average parameters for an assumed approximately homogeneous layer.

The presence of a layer of different permeability in an otherwise homogeneous system is seen to markedly affect the temperature difference required to destabilize the fluid (for the example presented, $r_1 = r_3 = 0{\cdot}4$, the factors are 0·017, 0·160, 0·701, 2·334, 4·764 and 4·920 for $K_2/K_1 = 1000$, 100, 10, 0·1, 0.01 and 0·001 respectively).

Streamlines and isotherm patterns for the permeability ratios $K_2/K_1 = 100$, 10, 0·1 and 0·01 are shown in figure 8. Most of the flow takes place in the more permeable layer(s). The isotherm patterns are not altered a great deal, however, from the homogeneous case, unless the permeability ratio is greatly different from 1.

As $K_2/K_1 \to 0$, the flow forms two separate cells in the upper and lower more permeable layers, separated by an almost impermeable layer. The flow patterns remain influenced by the conducting effect of the middle layer, which connects the upper and lower convection cells. (The isotherm pattern in figure 8*d* shows the influence clearly, for the case $K_2/K_1 = 0{\cdot}01$.)

7. Conclusions

The two- and three-layer examples considered above are by no means exhaustive. It is of interest to consider a very thin middle layer, for example. However they will serve to demonstrate the sort of phenomena which can occur in relation to the onset of convection in a layered porous medium. The results clearly show that very significant permeability differences are required to force the layered system into an onset mode different from that for a homogeneous system. Since such permeability differences do occur in hydrothermal systems, the problem has practical relevance.

The methods of analysis presented here are quite general and could be used to examine more complicated layered systems.

REFERENCES

Beck, J. L. 1972 *Phys. Fluids* **15**, 1377.
Caltagirone, J. P. 1975 *J. Fluid Mech.* **72**, 269.
Castinel, G. & Combarnous, M. 1975 *Rev. Thermique* **168**, 937.
Donaldson, I. G. 1962 *J. Geophys. Res.* **67**, 3449.
Elder, J. W. 1967 *J. Fluid Mech.* **27**, 29.
Epherre, J. F. 1975 *Rev. Thermique* **168**, 949.
Gheorghitza, St. I. 1961 *Proc. Camb. Phil. Soc.* **57**, 871.
Horton, C. W. & Rogers, F. T. 1945 *J. Appl. Phys.* **16**, 367.
Joseph, D. D. 1976 *Stability of Fluid Motions*. Springer.
Katto, Y. & Masuoka, T. 1967 *Int. J. Heat Mass Transfer* **10**, 297.
Lapwood, E. R. 1948 *Proc. Camb. Phil. Soc.* **44**, 508.
Nield, D. A. 1968 *Water Resources Res.* **4**, 553.
Prat, M. 1966 *J. Geophys. Res.* **71**, 4835.
Rana, R. 1977 M.Sc. thesis, Stanford University, California.
Ribando, R. J. & Torrance, K. E. 1976 *Trans. A.S.M.E.* C, *J. Heat Transfer* **98**, 42.
Schneider, K. J. 1963 *11th Int. Cong. Refrigeration, Munich*, Paper no. 11–4.

SCHUBERT, G. & STRAUS, J. M. 1977 *J. Geophys. Res.* **82**, 3411.

SCHUBERT, G. & STRAUS, J. M. 1978 *J. Fluid Mech.* **91**, 155.

STRAUS, J. M. 1974 *J. Fluid Mech.* **64**, 51.

STRAUS, J. M. & SCHUBERT, G. 1977 *J. Geophys. Res.* **82**, 325.

SUN, Z. S., TIEN, C. & YEN, Y. C. 1972 *Proc. Fourth Int. Heat Transfer Conf.*, (*Paris–Versailles*), vol. IV, paper NC2–11.

SUTTON, F. M. 1970 *Phys. Fluids* **13**, 1931.

TYVAND, P. A. 1977 *J. Hydrology* **34**, 335.

WESTBROOK, D. R. 1969 *Phys. Fluids* **12**, 1547.

WOODING, R. A. 1959 *Proc. Roy. Soc.* A **252**, 120.

WOODING, R. A. 1960 *J. Fluid Mech.* **9**, 183.

YEN, Y. C. 1974 *Int. J. Heat Mass Transfer* **17**, 1349.